

ISTITUTO NAZIONALE DI FISICA NUCLEARE

Sezione di Napoli

INFN/AE-97/56
10 Novembre 1997

G. Carlini:

SUSY SEARCHES AT LEP2 WITH THE L3 DETECTOR

To be published on: *Proceedings of "Lake Louise 1997 Winter Institute"*, February 16–22, 1997

SIS-Pubblicazioni
dei Laboratori Nazionali di Frascati

SUSY Searches at LEP2 with the L3 Detector

G. Carlino

University of Naples and INFN-Sezione di Napoli, Italy

Abstract

Searches of supersymmetric particles have been performed by the L3 experiment with data collected in the LEP run at centre of mass energy of 130–136 GeV in the autumn 1995 and at 161 and 172 GeV in the summer 1996 with an integrated luminosity of about 26 pb^{-1} . The preliminary results of our analysis are reported. No evidence of supersymmetric particles has been found and limits on the production cross section of charginos, neutralinos, stop quarks and scalar leptons have been set. Limits on the masses of the supersymmetric particles have been improved with respect to LEP1. New regions in the space of the MSSM parameters have been excluded.

1 Introduction

The precision measurements at LEP have given an extraordinary confirmation of the validity of the Standard Model up to the electroweak energy scale and there isn't any strong experimental indication for failure of this theory at higher energy. However, the Standard Model leaves many fundamental parameters unexplained such as the electroweak mixing parameter $\sin^2 \theta$. The quadratic divergences of scalar masses at the one-loop level and the large difference between the electroweak and the grand unification scales (hierarchy problem) are further problem of the Standard Model.

At present, one of the most attractive possibilities of extending the Standard Model is provided by Supersymmetry [1] (SUSY) which gives a solution to some of these questions. Supersymmetry predicts the existence of a "superpartner" to each ordinary particle, with the same mass and gauge quantum numbers, but with spin different by half a unit. However, supersymmetry is not an exact symmetry of the nature since otherwise light superpartners of the quarks and leptons would have been observed. The breaking of supersymmetry manifests itself via mass splitting between the particles and their superpartners. This mass splitting should be such that one expects SUSY particles to have masses below or about 1 TeV in order to solve the hierarchy problem. The possibility that some of the SUSY particles may have masses even much lower than this value and therefore be kinematically accessible at LEP2 has given a huge interest in experimental searches of supersymmetry.

The simplest supersymmetric extension of the Standard Model is the Minimal Supersymmetric Standard Model (MSSM) [2], based of the same $SU(3) \times SU(2) \times U(1)$ gauge symmetry group. It has the minimal particle content, containing, in addition to the known particles, their superpartners: gauginos ($\tilde{g}, \tilde{W}^\pm, \tilde{Z}, \tilde{\gamma}$), squarks \tilde{q} and sleptons \tilde{l} . The novelty is that the MSSM requires at least two Higgs doublets $H_1 = (H_1^0, H_1^-)$ and $H_2 = (H_2^+, H_2^0)$ to generate the masses of the gauge bosons and the fermions.

The charged gauginos \tilde{W}^\pm mix with the charged higgsinos to form two charged mass eigenstates: the charginos $\tilde{\chi}_1^\pm$ and $\tilde{\chi}_2^\pm$. The neutral gauginos \tilde{Z} and $\tilde{\gamma}$ and the neutral higgsinos mix to form four neutral mass eigenstates: the neutralinos $\tilde{\chi}_1^0, \tilde{\chi}_2^0, \tilde{\chi}_3^0$ and $\tilde{\chi}_4^0$ in order of increasing mass.

To the two chirality states of the charged leptons and quarks correspond the right and left scalar particles $\tilde{\ell}_R, \tilde{\ell}_L$ and \tilde{q}_R, \tilde{q}_L . The left and right scalar particles mix and the mixing is assumed to be proportional to the corresponding fermionic Yukawa coupling. The scalar partners of the light fermions, \tilde{f}_L, \tilde{f}_R , are to a good approximation mass eigenstates, whereas the mass eigenstates can have large mass splitting for the sbottom and the stop quarks. Due to the high mass of the top quark, stop quarks can be much lighter than all other squarks [3]. The lightest stop mass eigenstate: $\tilde{t}_1 = \tilde{t}_L \cos \theta_{LR} + \tilde{t}_R \sin \theta_{LR}$ may be the lightest supersymmetric charged particle [4].

The mechanism for the chargino production in the e^+e^- annihilation is the γ and Z exchange in the s channel and $\tilde{\nu}$ exchange in the t channel with a destructive interference. The influence

of the second diagram is relevant if the $\tilde{\nu}$ is light and the chargino is gaugino-like (the higgsino-like chargino doesn't couple to the sneutrino). Therefore the chargino production cross section is independent from $m_{\tilde{\nu}}$ for an higgsino-like chargino whereas for a gaugino-like chargino is large (of the order of several pb) for large sneutrino mass and it is sensibly reduced for small $m_{\tilde{\nu}}$.

If the masses of the H^\pm , $\tilde{\ell}$ and $\tilde{\nu}$ are very high, the $\tilde{\chi}^\pm$ decays via virtual W into $\tilde{\chi}_1^\circ \ell^\pm \nu$ and $\tilde{\chi}_1^\circ q \bar{q}'$. If the slepton and the sneutrino masses are comparable with the W mass the leptonic branching ratio is enhanced. The 2-body decays $\tilde{\chi}^\pm \rightarrow \tilde{\ell} \nu, \ell \tilde{\nu}$ are dominant if kinematically allowed.

The neutralino production in the process $e^+e^- \rightarrow \tilde{\chi}_1^\circ \tilde{\chi}_2^\circ$ proceeds via Z exchange in the s channel and $\tilde{e}_{L,R}$ exchange in the t and u channel. The Z couples only to the higgsino components of the neutralino and the selectron couples only to the gaugino components. The cross section is sufficiently large for the higgsino-like neutralino and we have sizeable cross section for a gaugino-like one only if $m_{\tilde{e}} \simeq m_Z$. The decays $\tilde{\chi}_2^\circ \rightarrow \tilde{\chi}_1^\circ f \bar{f}$ proceed mainly via Z exchange. As for the chargino decays, virtual sleptons and sneutrino exchange may enhance the leptonic branching ratio.

Sleptons are produced in Z/γ exchange in the s channel and, only for the selectron, in the t channel via the $\tilde{\chi}^\circ$ exchange. The process $e^+e^- \rightarrow \tilde{e}_L^\pm \tilde{e}_R^\mp$ receives only the t channel contributions. The cross section of the selectron production is larger with respect to the other sleptons because of the t channel contributions. The main slepton decay channel is $\tilde{\ell} \rightarrow \tilde{\chi}_1^\circ \ell$.

The stop quarks are produced in the s channel via Z/γ exchange. The \tilde{t} coupling to the Z and the production cross section depend on the mixing angle θ_{LR} . The cross section has a maximum for $\cos \theta_{LR} = 1$. The main stop decay is the process $\tilde{t} \rightarrow \tilde{\chi}_1^\circ c$.

2 SUSY signature

An important assumption usually made in the MSSM is the existence of a discrete symmetry, called R -parity, which distinguishes the ordinary particles ($R = 1$) from their supersymmetric partners ($R = -1$).

The R -parity conservation restricts the possible interactions of the theory: at every vertex there must be an even number of supersymmetric particles. As a consequence, SUSY particles are produced in pairs and the Lightest Supersymmetric Particle (LSP) is stable and, hence, will contribute to the dark matter of the universe.

From astrophysical considerations [5] the LSP must be neutral and colourless restricting the possible choices to the lightest neutralino, the sneutrino or the gravitino. In the following we assume that $\tilde{\chi}_1^\circ$ is the LSP.

The $\tilde{\chi}_1^\circ$ behaves as a heavy neutrino escaping the detector and leaving an unbalanced momentum and missing energy in the observed event. The common signature of all the SUSY events is therefore an excess of missing energy, large missing transverse momentum and large

acoplanarity.

Different final state topologies arise from the production of charginos, neutralinos, sleptons and stops. The chargino production $e^+e^- \rightarrow \tilde{\chi}_1^+ \tilde{\chi}_1^-$ signature depends on whether both, only one, or neither of the two charginos decay leptonically. The final state topologies are respectively: two acoplanar leptons, not necessarily of the same flavour, plus missing energy, one isolated lepton plus jets and missing energy and an hadronic system with missing energy. The neutralino production $e^+e^- \rightarrow \tilde{\chi}_1^0 \tilde{\chi}_2^0$, followed by $\tilde{\chi}_2^0 \rightarrow \tilde{\chi}_1^0 f \bar{f}$, leads to final states consisting of a lepton pair or two hadronic jets plus missing energy. Slepton pairs are identified by two acoplanar leptons of the same flavour and stop pair production signature, followed by $\tilde{t} \rightarrow \tilde{\chi}_1^0 c$, is the presence of two acoplanar jets.

All these processes lead to three common final state topologies: the hadronic topology HH for the hadronic events with missing energy, the semileptonic topology LH for events with an isolated lepton in hadronic environment with missing energy and the leptonic topology LL for events with acoplanar leptons and small multiplicity in presence of missing energy. The LL topology is designed for the slepton pair searches and for the chargino and neutralino searches when both the charginos and the $\tilde{\chi}_2^0$ decay leptonically. The LH topology is used especially in the chargino searches with an hadronic and a leptonic chargino decay and the HH topology for all the other processes.

For each topology it has been designed a dedicated analysis. Moreover, because of the different background processes involved, we used distinct strategies depending on the value of the parameter ΔM , defined as the mass difference between the SUSY particle and the LSP.

3 Background processes

All the physical processes with missing energy are background for the SUSY searches. The missing energy being produced either by neutrinos or by undetected particles going in the beam-pipe or in the region not covered by the detector.

The main background sources can be grouped in four categories:

- two photon interactions $e^+e^- \rightarrow e^+e^- f \bar{f}$, with a large cross section divergent with the invariant mass of the photon pair $M_{\gamma\gamma}$;
- s channel electroweak processes $e^+e^- \rightarrow Z/\gamma^* \rightarrow f \bar{f}$, mainly the “radiative return” to the Z and the tau pairs production;
- W pairs production $e^+e^- \rightarrow W^+W^-$;
- t channel electroweak processes $e^+e^- \rightarrow W e \nu, Z/\gamma^* Z^*/\gamma^*, Z e e$ with small cross sections compared to the previous processes.

In the small ΔM region ($\Delta M < 15$ GeV) the dominant background source is the two photon physics. In the large ΔM region ($\Delta M > 40$ GeV) W pairs production is the most offending background, especially for heavy LSP.

4 Data sample and simulation

In our analysis we use the data collected by the L3 detector [6] during the high energy run of LEP in November 1995 at $\sqrt{s} = 130, 136$ GeV, corresponding to an integrated luminosity of 5.1 pb^{-1} , and in the summer 1996 at $\sqrt{s} = 161$ and $\sqrt{s} = 172$ GeV corresponding respectively to integrated luminosities of 11.1 and 10.2 pb^{-1} .

Signal events have been generated with the program SUSYGEN [7]. For charginos, events have also been generated with the program DFGT [8], which takes into account the spin correlation between the charginos. Stop quark events have been generated using a dedicated event generator [9]. In every case, we have generated a grid of points in the space $(M_{sp}, \Delta M)$, where M_{sp} is the mass of the supersymmetric particle, each containing about 1000 events. Monte Carlo simulated events for the main background sources have been produced at all the centre of mass energies. The number of simulated events for the background is equivalent to about 10 times the statistics of the collected data. We use PYTHIA [10] to simulate all the backgrounds except Bhabha events, simulated with BHAGENE [11], $e^+e^- \rightarrow l^+l^-(\gamma)$, simulated with KORALZ [12], and $e^+e^- \rightarrow W^+W^-$, simulated with EXCALIBUR [13]. The two photon interactions have been simulated also with PHOJET [14] and DIAG36 [15]. The trigger of the L3 detector has been simulated for all the sub-detectors in order to study in details the trigger efficiency. A precise simulation of the trigger efficiency is crucial for the events with small ΔM since the heavy neutralinos carry away a large fraction of the energy of the event reducing the visible energy in the detector.

5 The Analysis strategy

The aim of our analysis is, of course, the discovery of a supersymmetric signal. In order to have a positive result in our searches we developed a two steps analysis strategy. In the beginning, during the data taking, we applied some very loose selections for the chargino, neutralino, sleptons and stop searches in order to have a large signal efficiency regardless of the background selected and to detect any small discrepancy between data and Monte Carlo.

For every supersymmetric process under study we defined different selections depending on the final state topology (HH , LH and LL) and the ΔM range. All the selections being applied in OR. A description of the variables used in the selections can be found, for example, in the reference [16].

We didn't observe any significant discrepancy between data and Monte Carlo apart from a

small data excess in the large ΔM region in the hadronic and semileptonic selections. As no evidence of Supersymmetry has been found we applied the second step of our analysis strategy where the selections have been tightened and optimised in order to derive the best upper limits on the production cross sections of the supersymmetric particles.

The optimisation procedure of each selection varies all the cuts over the Monte Carlo variables simultaneously in order to have the highest possible sensitivity for the signal. The search sensitivity is optimised minimising the ratio between the average Poisson upper limit on the signal, with background subtraction, and the signal efficiency: $\sum_{n=0}^{\infty} k_n P_b(n)/\varepsilon$, where k_n is the 95% C.L. Poisson upper limit for n observed events, $P_b(n)$ is the Poisson distribution for observing n events with a background of b events (estimated from Monte Carlo) and ε is the average efficiency [16, 17]. All the optimised selections corresponding to a given SUSY process, final state topology and ΔM range are applied in logical OR and only those selections giving a minimum of the sensitivity function are chosen for the final selection.

6 The Results

In the following the preliminary results of the L3 analysis are presented. When we apply the final global selection the total number of expected Monte Carlo background events is about 7.6, of which 3.4 are given to the two photon interactions in the small ΔM range. We don't subtract this background in the limits derivation because the shapes of the distributions of the variable used in the selections are not reproduced very precisely in the Monte Carlo simulation.

The total number of events selected is 8, of which none at $\sqrt{s} = 130, 136$ GeV, 1 at $\sqrt{s} = 161$ GeV and 7 at $\sqrt{s} = 172$ GeV.

The details of the selections of the single processes analysed are the following: the total number of events selected and the number of expected background events for the chargino and neutralino selection is respectively 5 and 3.7, for the slepton selection 4 and 3.5 (all the events are selected in the selectron channel) and for the stop selection 1 and 1.5.

The selection efficiency for all the processes shows a maximum in the intermediate ΔM region and drops in the large and small ΔM regions because of the WW and the two photon background respectively. In the small ΔM region the efficiency is also reduced because of the trigger inefficiency (the average trigger efficiency is about 75% at $\Delta M = 5$ GeV and 100% for $\Delta M > 10$ GeV). In the figure 1a, as an example, is shown the selection efficiency for the chargino detection in the chargino and neutralino mass plane. 100% W branching ratio is assumed. The neutralino, sleptons and stop signals have comparable efficiencies with similar trends.

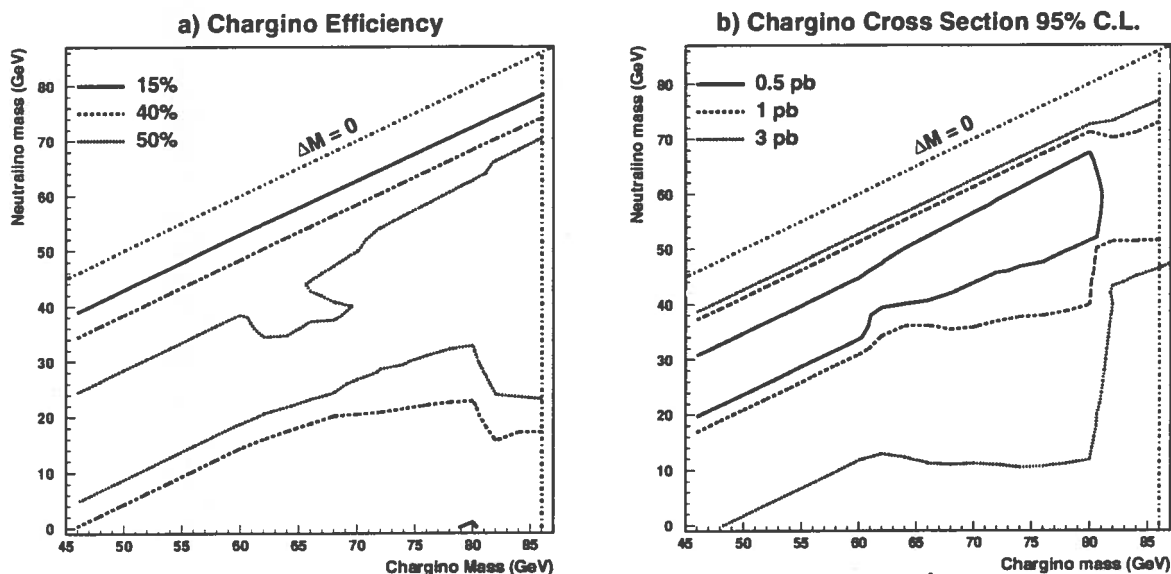


Figure 1: a) Efficiency for chargino detection and b) 95% C.L. upper limits in the chargino production cross section assuming 100% W branching ratio.

6.1 Limits on production cross section

Given the signal efficiency ε_s , the integrated luminosity \mathcal{L} , the number of selected events N_0 and the expected background μ_b , it is possible to set the 95% C.L. upper limit on the production cross sections of all the supersymmetric particles. The limit is given by $\sigma = N_s/\varepsilon_s\mathcal{L}$ where N_s is the upper limit to the number of signal events [18].

In figure 1b is shown the 95% C.L. upper limit on the production cross section for a chargino with mass in the range between 45 and 86 GeV. In the limit derivation the W branching ratio is assumed and the data at all the centre of mass energies are combined.

6.2 Interpretation in the MSSM

In the MSSM, supersymmetry breaking is determined by a set of “soft breaking” mass terms. Among these are the gaugino masses M_1 , M_2 and M_3 , associated to the gauge groups $U(1)$, $SU(2)$ and $SU(3)$. These mass terms are assumed to be equal at the unification scale, leading to $M_1 = 5/3M_2 \tan^2 \theta_W$ at the electroweak scale. In the MSSM the spectrum of the masses of the gauginos and of the supersymmetric particles is entirely described by four parameters: $\tan \beta$, $M \equiv M_2$, μ and m_0 .

The $\tan \beta$ parameter is the ratio of the vacuum expectation values of the two higgs doublets, μ is the higgsino mixing parameter and m_0 is the common scalar mass at the grand unification scale [19].

The parameters M , μ and $\tan \beta$ determine the field contents of charginos and neutralinos as

a mixing of gauginos and higgsinos. The m_0 parameter determines the mass spectrum of the scalar particles at the electroweak scale. A light m_0 results in low values of the masses of the sleptons and the sneutrino, thereby enhancing the t channel in the chargino production and reducing the cross section. On the other hand, high values of m_0 decouple the $\tilde{\nu}$ from the theory enhancing the chargino production rate. In the following we will consider $m_0 = 500$ GeV and $\tan \beta \geq 1$.

The results of the L3 analysis may be expressed as mass limits and exclusion of regions in the MSSM parameter space. In the figure 2 is shown the excluded region at 95% C.L. in the $M - \mu$ plane resulting from the combined searches for charginos and neutralinos for $\tan \beta = 1.41$ and $\tan \beta = 40$ computed for $m_0 = 500$ GeV. As shown in the figure the kinematical limits for the chargino production has been reached in almost all the planes. The region excluded with the LEP2 data improves significantly the results of LEP1 [20].

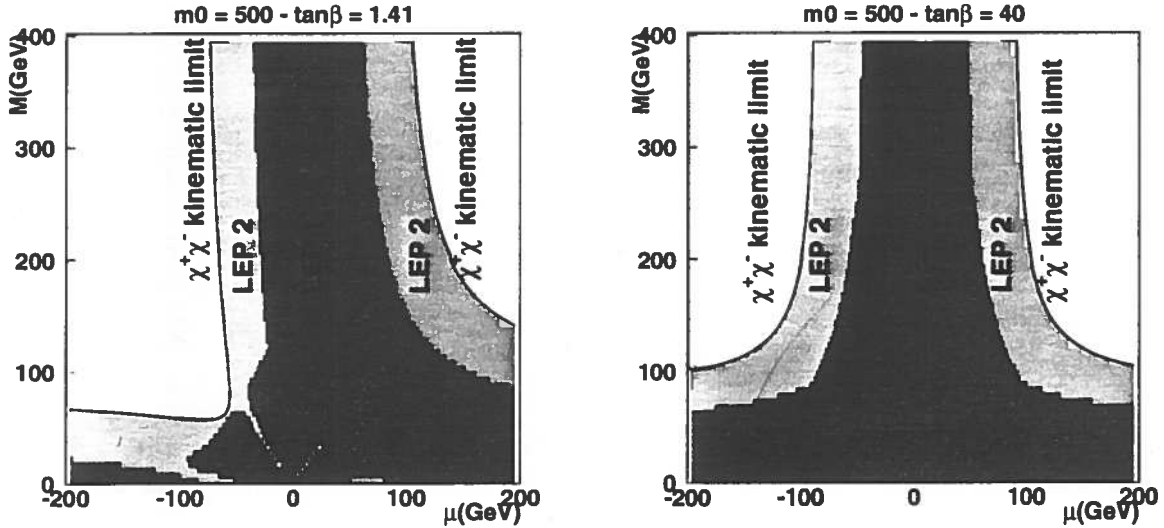


Figure 2: Excluded regions in the (M, μ) plane for $\tan \beta = 1.41$ and 40 with $m_0 = 500$ GeV. The light (dark) shaded areas are the region excluded at LEP2 (LEP1). The kinematical boundary at $\sqrt{s} = 172$ GeV for $\tilde{\chi}_1^+ \tilde{\chi}_1^-$ production is shown by the solid lines.

The lower limit on the lightest neutralino mass can be obtained from the exclusion regions in the $M - \mu$ plane. The limit is derived scanning the regions not excluded by LEP1 and LEP2 and taking the lower value of the lightest neutralino mass. In the figure 3 is shown the $\tilde{\chi}_1^0$ mass limit as a function of $\tan \beta$. For low $\tan \beta$ the LEP1 results alone cannot rule out a massless neutralino and the LEP2 data alone give a mass limit of less the 10 GeV. With the combination of the LEP1 and LEP2 results we can set the limit: $M_{\tilde{\chi}_1^0} \geq 24.6$ GeV for $m_0 = 500$ GeV.

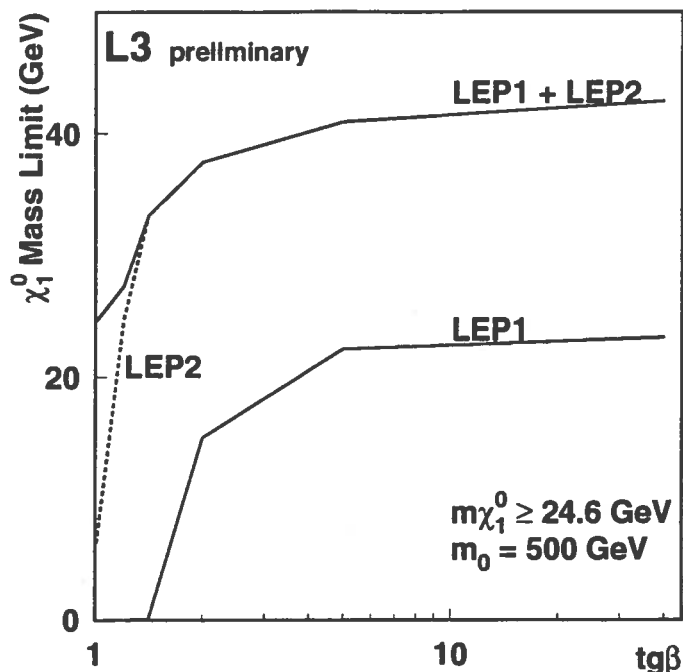


Figure 3: Lower limit on the mass of the lightest neutralino as a function of $\tan\beta$ for $m_0 = 500$ GeV. The limits of LEP1 and LEP2 and the combined results are shown.

Figure 4 shows the 95% C.L. exclusion regions in the planes $M_{\tilde{\chi}_1^\pm} - M_{\tilde{\chi}_1^0}$ and $M_{\tilde{\chi}_2^0} - M_{\tilde{\chi}_1^0}$, computed for $\tan\beta = 1.41$ and 40 with $m_0 = 500$ GeV, corresponding to the exclusion regions in the plane $M - \mu$. The accessible region is limited by the MSSM. For the chargino almost all the accessible region of mass space before the kinematical limit is excluded whereas for the neutralino not as much of the accessible region is excluded because of the smaller predicted cross section. The small excluded region beyond the kinematical limit $M_{\tilde{\chi}_2^0} + M_{\tilde{\chi}_1^0} = 172$ GeV is due to the chargino searches.

The results of the slepton analysis are summarised in the figure 5a. The excluded regions in the plane $M_{\tilde{l}_R} - M_{\tilde{\chi}_1^0}$ from the direct search of the selectron and smuon production for $\mu = -200$ and $\tan\beta = 1.41$ are shown. The exclusion limit for the selectron production is larger than for the smuon because of the larger selectron cross section due to the t channel contribution. In the figure is also shown the excluded region derived from the neutralino and chargino searches in the framework of the MSSM for the given parameters.

Limits from the stop quark direct search are shown in the figure 5b in the stop and neutralino mass plane as function of the mixing angle $\cos\theta_{LR}$. The stronger limit is given by $\cos\theta_{LR} = 1$ where the maximum cross section is expected. The worst limit is obtained for $\cos\theta_{LR} = 0.57$ where the stop decouples completely from the Z and can be produced only via the γ exchange. The limits set on the stop mass for $\Delta M > 10$ GeV are: $M_{\tilde{t}_1} > 68.9$ GeV for $\cos\theta_{LR} = 1$ and $M_{\tilde{t}_1} > 58.3$ GeV for any $\cos\theta_{LR}$.

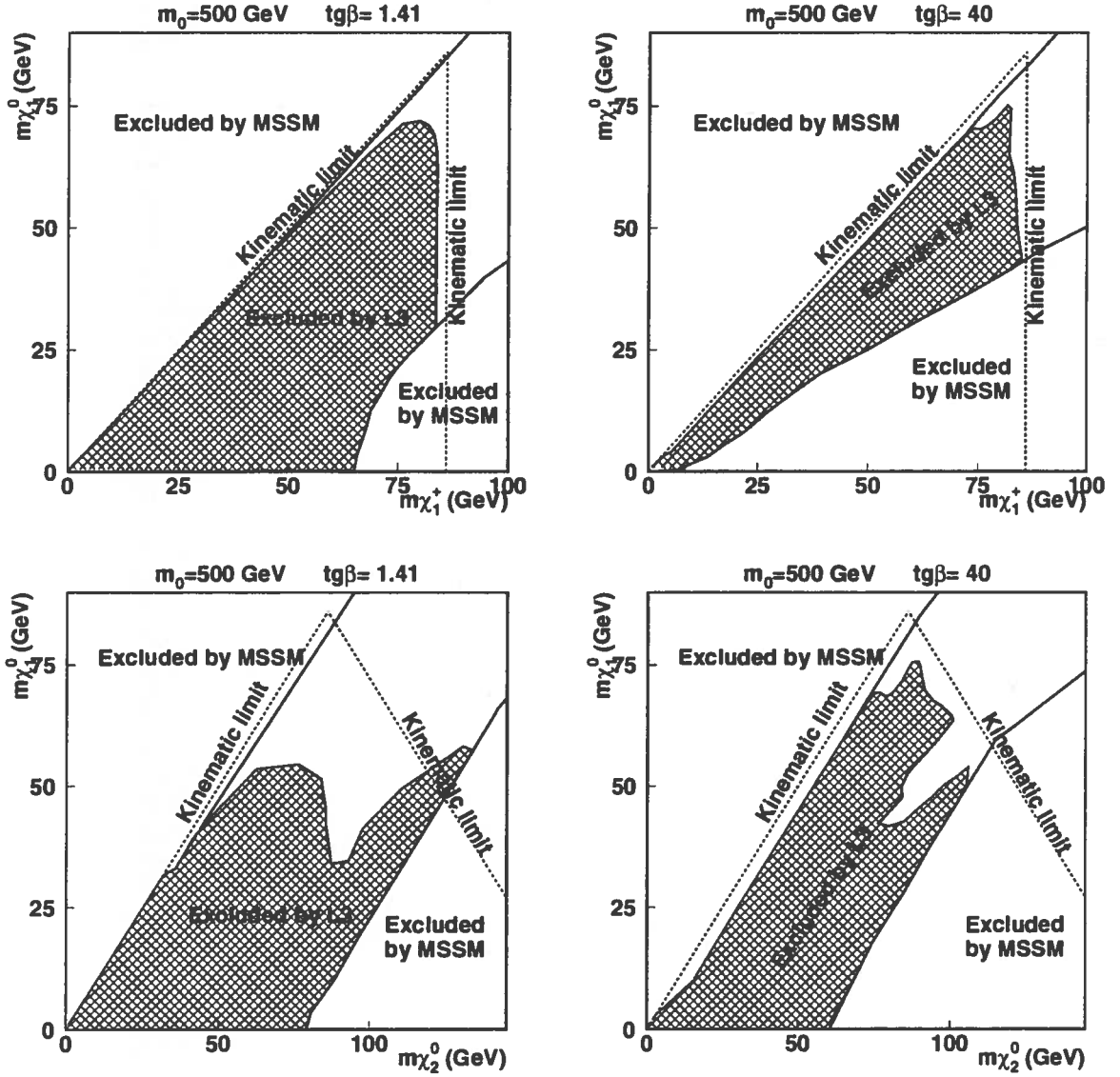


Figure 4: The 95% C.L. excluded regions in the $M_{\tilde{\chi}_1^\pm} - M_{\tilde{\chi}_1^0}$ and $M_{\tilde{\chi}_2^0} - M_{\tilde{\chi}_1^0}$ planes within the framework of the MSSM for $m_0 = 500$ GeV and $\tan\beta = 1.41$ and 40 . The solid lines represent the theoretical bounds of the MSSM parameter space. The kinematical boundaries at $\sqrt{s} = 172$ GeV are shown by dashed lines.

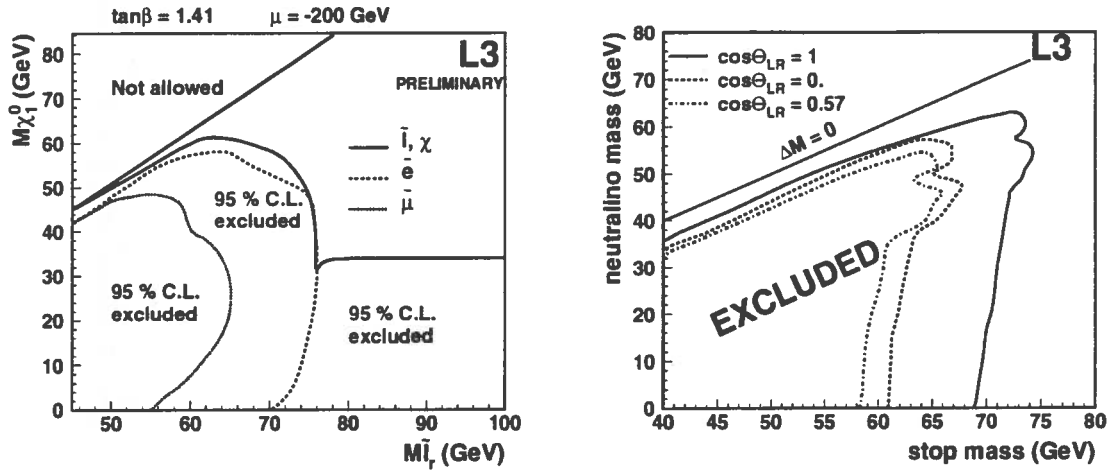


Figure 5: The 95% C.L. excluded regions a) in the slepton neutralino mass plane and b) in the stop neutralino mass plane for different values of $\cos\theta_{LR}$.

7 Conclusion

A search for charginos, neutralinos, sleptons and stop quarks has been performed by the L3 experiment with data collected at $\sqrt{s} = 130$ – 136 , 161 and 172 GeV. No evidence of SUSY particles has been found and upper limits on the production cross sections have been set. In the framework of the MSSM, improved mass limits have been set and new regions in the space of the supersymmetric parameters have been excluded with respect to LEP1. The kinematically accessible region for chargino production has been almost completely excluded and the limit on the lightest neutralino mass of 26.4 GeV has been set. The sleptons and stop quark mass limits have been improved with respect to LEP1. The results shown have to be considered as preliminary.

Acknowledgments

I would like to express my thanks to all the L3 SUSY working group members, and in particular to Carlo Dionisi, Salvatore Mele, Hanna Nowak, Marco Pieri and Sylvie Rosier-Lees, for the help they gave me in the preparation of this talk.

References

- [1] Y.A. Goldfand and E.P.Likhtman, *JETP Lett* **13** (1971) 323;
D.V. Volkhov and V.P. Akulov, *Phys. Lett.* **B46** (1973) 109;
J.Wess and B.Zumino, *Nucl. Phys.* **B70** (1974) 39;
P.Fayet and S.Ferrara, *Physics Reports* **32** (1977) 249.

- [2] H.E.Haber and G.Kane, *Physics Reports* **117** (1985) 75;
H.P.Nilles, *Physics Reports* **110** (1984) 1;
R.Barbieri, *Riv. Nuovo Cimento* **11 no. 4** (1988) 1.
- [3] S.Abachi *et al.*, *Phys. Rev. Lett.* **74** (1995) 2632;
F.Abe *et al.*, *Phys. Rev. Lett.* **74** (1995) 2626.
- [4] A. Bouquet *et al.* *Nucl. Phys.* **B262** (1985) 299;
J.Ellis and S.Rudaz, *Phys. Lett.* **B128** (1983) 248.
- [5] J.Ellis, J.S. Hagelin, D.V. Nanopoulos, K. Olive and M. Srednicki, *Nucl. Phys.* **B238** (1984) 453.
- [6] B.Adeva *et al.* (L3 collab.) *Nucl. Instrum. Methods* **A289** (1990) 35;
O.Adriani *et al.* (L3 collab.) *Physics Reports* **236** (1993) 1.
- [7] S. Katsanevas and M. Melachroinos, "SUSYGEN generator" in "Physics at LEP2", CERN 96-01 Vol.2 (1996) 328.
- [8] C.Dionisi, K.Fujii, S.Giagu and T.Tsukamoto, "DFGT generator" in "Physics at LEP2", CERN 96-01, vol.2 (1996) 337.
- [9] A. Sopczak, L3 Note 1860, in "Physics at LEP2", CERN 96-01 Vol.2 (1996), 343.
- [10] T. Sjöstrand, *Comp. Phys. Comm* **82** (1994) 74.
- [11] J.H. Field, *Phys. Lett.* **B323** (1994) 432.
- [12] S.Jadach, B.F.L.Ward and Z.Was, *Comp. Phys. Comm* **79** (1994) 503.
- [13] F.A. Berends, R.Pittau, R.Kleiss *Comp. Phys. Comm* **85** (1995) 437.
- [14] E. Boudinov *et al.*, " $\gamma\gamma$ Event Generator", hep-ph/9512371 (1995).
- [15] F.A.Berends *et al.*, *Nucl. Phys.* **B253** (1985) 441.
- [16] M.Acciari *et al.* (L3 collab.), *Phys. Lett.* **B377** (1996) 289.
- [17] J.F. Grivaz, F. Le Diberder, preprint LAL-92-37, June 1992.
- [18] Review of Particle and Fields, *Phys. Rev.* **D54** (1996) 1.
- [19] A.Bartl *et al.*, *Z. Phys.* **C55** (1992) 257;
S.Ambrosiano and B.Mele, *Phys. Rev.* **D52** (1995) 3900;
A.Bartl, H.Fraas and W.Majerotto *Z. Phys.* **C34** (1987) 411;
S.Ambrosiano and B.Mele, *Phys. Rev.* **D53** (1996) 2541.
- [20] M.Acciari *et al.* (L3 collab.) *Phys. Lett.* **B350** (1995) 109.